

See discussions, stats, and author profiles for this publication at: <https://www.researchgate.net/publication/234051230>

Synthesis, characterization, optical absorption, luminescence and defect centres in Er³⁺ and Yb³⁺ co-doped MgAl₂O₄ phosphors

ARTICLE in APPLIED PHYSICS B · MARCH 2012

Impact Factor: 1.86 · DOI: 10.1007/s00340-012-4970-4

CITATIONS

5

READS

88

7 AUTHORS, INCLUDING:



V. Singh

116 PUBLICATIONS 959 CITATIONS

[SEE PROFILE](#)



Dr. Vineet Kumar Rai

Indian School of Mines

107 PUBLICATIONS 1,040 CITATIONS

[SEE PROFILE](#)



Gundu Rao

University of São Paulo

118 PUBLICATIONS 1,400 CITATIONS

[SEE PROFILE](#)



Y. D. Jho

Gwangju Institute of Science and Technology

110 PUBLICATIONS 459 CITATIONS

[SEE PROFILE](#)

Synthesis, characterization, optical absorption, luminescence and defect centres in Er^{3+} and Yb^{3+} co-doped MgAl_2O_4 phosphors

V. Singh · V. Kumar Rai · S. Watanabe ·
T.K. Gundu Rao · L. Badie · I. Ledoux-Rak · Y.-D. Jho

Received: 12 November 2011
© Springer-Verlag 2012

Abstract The $\text{Er}^{3+}\text{-Yb}^{3+}$ co-doped MgAl_2O_4 phosphor powders have been prepared by the combustion method. The phosphor powders are well characterized by X-ray diffraction (XRD) and energy dispersive (EDX) techniques. The absorption spectrum of $\text{Er}^{3+}/\text{Er}^{3+}\text{-Yb}^{3+}$ doped/co-doped phosphor powder has been recorded in the UV–Vis–NIR region of the electro-magnetic spectrum. The evidence for indirect pumping under 980 nm excitation of Er^{3+} from Yb^{3+} was observed in the MgAl_2O_4 matrix material. Electron spin resonance (ESR) studies were carried out to identify the defect centres responsible for the thermally stimulated luminescence (TSL) process in $\text{MgAl}_2\text{O}_4:\text{Er}^{3+}$ phosphor. Three defect centres were identified in irradiated phosphor by ESR measurements which were carried out at room temperature and these were assigned to an O^- ion and F^+ centres. O^- ion (hole centre) appears to correlate with the low tempera-

ture TSL peak at 210 °C and one of the F^+ centres (electron centre) is related to the high temperature peak at 460 °C.

1 Introduction

Magnesium aluminate (MgAl_2O_4) phosphor can show efficient luminescence in the presence of certain suitable dopants, particularly rare earths, in the lattice [1–4]. Phosphors, especially doped with Er and Yb rare-earth ions, are widely reported in the literature and have been used in visible up-conversion lasers and efficient NIR lasers [5–8]. The process of energy transfer from Yb^{3+} to other activators (rare earth ions) has been studied by many authors and Yb^{3+} has been found as an efficient sensitizer for other rare earth ions such as trivalent Tm, Ho, and Er for the futuristic photonic applications [9–11]. Enhancement in the fluorescence efficiency due to the Yb^{3+} ions was reported in several Er^{3+} -doped phosphor materials [12–14]. Even though several investigations based on rare-earth and transition metal ions doped MgAl_2O_4 are available [1–4, 15–19], studies based on $\text{MgAl}_2\text{O}_4:\text{Er}^{3+}$ phosphor powders co-doped with Yb^{3+} have not yet been investigated in detail. The Er^{3+} doped materials are playing a significant role in the development of photonic devices due to the commercialization of the 980 nm laser diode. Near-infrared luminescence and laser emission of Er^{3+} doped materials at 1.5 μm is of great interest for optoelectronics engineers and material scientists in recent years due to its role in fiber optical communication and many other applications [20–23]. Much work has concentrated on the nature and symmetry of the erbium centre responsible for 1.5 μm emission in solid host with sometimes contradictory results. Therefore, luminescence studies must be combined with electron spin resonance (ESR) for

V. Singh (✉) · Y.-D. Jho
School of Information and Communications, Gwangju Institute of
Science and Technology, Gwangju 500-712, South Korea
e-mail: vijayjiin2006@yahoo.com

Y.-D. Jho (✉)
e-mail: jho@gist.ac.kr

V. Kumar Rai
Department of Applied Physics, Indian School of Mines,
Dhanbad 826004, India

S. Watanabe · T.K. Gundu Rao
Institute of Physics, University of Sao Paulo, 05508-090,
Sao Paulo, SP, Brazil

L. Badie · I. Ledoux-Rak
Laboratoire de Photonique Quantique et Moléculaire, Ecole
Normale Supérieure de Cachan, 61 av. du President Wilson,
94 235, Cachan, France

the full identification of the exact nature of trapping centres/defects. The knowledge of defects/traps and their distribution in the band gap of a solid host are very essential in order to understand the luminescence process of materials and to use them in various applications.

It is well established that the defect centres created by ionizing radiations such as alpha, beta, and gamma are responsible for thermally stimulated luminescence (TSL) in the phosphor. Electron spin resonance provides a convenient and sensitive technique for the identification and characterization of the defect centres. During the past decade, defect centres induced by radiation were studied using the techniques of TSL and ESR in rare-earth activated phosphate, mixed sulphate, and alkaline earth borate phosphors [24–28]. Recently, we have also combined ESR and TSL data to obtain information about the identification and decay of defect centres in the rare-earth doped aluminate, sulphide, and oxide phosphors [29–32].

In the present investigation, we have synthesized $\text{MgAl}_2\text{O}_4:\text{Er}^{3+}$ phosphor co-doped with the Yb^{3+} by the combustion method and characterized the phosphor using powder X-ray diffraction (PXRD) and energy-dispersive X-ray (EDX) analysis. The photoluminescence (PL) and thermally stimulated luminescence (TSL) studies on these phosphor powders have been carried out to investigate the effect of energy transfer from Yb^{3+} to Er^{3+} ion. The Photoluminescence (PL) and TSL intensity of Er^{3+} have been found to increase by the presence of Yb^{3+} in the co-doped MgAl_2O_4 host matrix, thus indicating an efficient energy transfer from Yb^{3+} to Er^{3+} . In addition, we have studied the defect centres formed in $\text{MgAl}_2\text{O}_4:\text{Er}^{3+}$ phosphor and Yb^{3+} co-doped phosphor using the ESR technique. The purpose of this work is to investigate correlations between ESR and thermally stimulated luminescence in $\text{MgAl}_2\text{O}_4:\text{Er}^{3+}$ phosphor co-doped with Yb^{3+} ions.

2 Experimental details

$\text{MgAl}_2\text{O}_4:\text{Er}_{(0.05)}$ {prepared using [Aluminum nitrate (10 g, $\text{Al}(\text{NO}_3)_3 \cdot 9\text{H}_2\text{O}$, ACROS], [Magnesium nitrate (3.4176 g, $\text{Mg}(\text{NO}_3)_2 \cdot 6\text{H}_2\text{O}$, Panreac], [Urea (5.4315 g, $\text{CH}_4\text{N}_2\text{O}$, Panreac], Erbium nitrate [0.2954 g, $\text{Er}(\text{NO}_3)_3 \cdot 5\text{H}_2\text{O}$, ACROS]} and $\text{MgAl}_2\text{O}_4:\text{Er}_{(0.05)}\text{Yb}_{(0.06)}$ {prepared using [Aluminum nitrate (10 g, $\text{Al}(\text{NO}_3)_3 \cdot 9\text{H}_2\text{O}$, ACROS], [Magnesium nitrate (3.4176 g, $\text{Mg}(\text{NO}_3)_2 \cdot 6\text{H}_2\text{O}$, Panreac], [Urea (5.5516 g, $\text{CH}_4\text{N}_2\text{O}$, Panreac], Erbium nitrate [0.2954 g, $\text{Er}(\text{NO}_3)_3 \cdot 5\text{H}_2\text{O}$, ACROS], Ytterbium nitrate [0.2871 g, $\text{Yb}(\text{NO}_3)_3 \cdot x\text{H}_2\text{O}$, Alfa Aesar]} were prepared by using the solution combustion method. The starting materials were dissolved in a minimum quantity of deionized water in 300 ml capacity Pyrex dish. The dish was inserted into a preheated furnace maintained at 550 °C. Within minutes, the

solution foamed and a flame was produced which lasted for several seconds. The dish was immediately removed from the furnace. The products obtained by combustion process were fluffy masses and these were crushed into a fine powder. The product of combustion reaction was then given an annealing treatment at 800 °C for 2 h in air to remove the thermal stress and impurities during its preparation and this was used for further characterization.

The phase composition of the synthesized powder was analyzed by XRD using Cu K α radiation (Bruker D8 Advance) in the 2 θ range of 10° to 80°.

The powders were taken onto a silicon stub with ethanol for their electron microscopic evaluation. After some time, the powders were coated with carbon and were observed using SEM (S-3400, Hitachi, Japan). Their chemical compositions were analyzed using the EDX attached to the SEM.

The UV-Vis-NIR absorption of the samples was measured at room temperature by diffuse reflectance spectroscopy using a Cary 6000i UV-Vis-NIR spectrometer equipped with an integrating sphere. The photoluminescence emission spectrum was studied using a Jobin-Yvon TRIAX 180 monochromator with a 150 grooves/mm grating coupled to a multi-channel InGaAs CCD detector. Samples were pumped by a diode (CW) laser operating at ~980 nm within the power range of 0 to 1 W.

Irradiation of the samples was carried out using a ${}^{60}\text{Co}$ gamma source. A Daybreak 1100 series automated TL reader system was utilized for TSL experiments which were carried out in a nitrogen atmosphere with a heating rate of 5 °C/sec. Electron Spin Resonance experiments were carried out using a Bruker EMX ESR spectrometer operating at X-band frequency with 100 kHz modulation frequency. Diphenyl Picryl Hydrazyl (DPPH) was used for calibrating the g-factors of defect centres. Temperature dependence of the ESR spectra was studied using a Bruker B VT 2000 variable temperature accessory.

3 Results and discussion

3.1 X-ray diffraction

The phase purity and crystal structure of the solution combustion synthesized samples were analyzed using the PXRD pattern. The PXRD patterns of the phosphors $\text{MgAl}_2\text{O}_4:\text{Er}^{3+}$ and $\text{MgAl}_2\text{O}_4:\text{Er}^{3+},\text{Yb}^{3+}$ are shown in Fig. 1. All the reflections of $\text{MgAl}_2\text{O}_4:\text{Er}^{3+}$ and $\text{MgAl}_2\text{O}_4:\text{Er}^{3+},\text{Yb}^{3+}$ could be indexed to those of standard MgAl_2O_4 (JCPDS No. 77-0435). It was noticed that the introduction of Er (5 %) does not create any other impurity phases, whereas extra loading of Yb (6 %) creates extra weak peaks at $2\theta \approx 29.8^\circ$ and $2\theta \approx 33.4^\circ$ that corresponds to Yb_2O_3 (JCPDS No. 84-1879) and YbAlO_3 (JCPDS No. 48-1633), respectively. Recently, Pošarac et al. [33] also observed the impurity phases

of Y_2O_3 and YAlO_3 in the combustion synthesized magnesium aluminate spinel doped with yttria. However, in the

present investigation, for both of the samples, PXRD patterns indicate that there is a formation of the spinel phase.

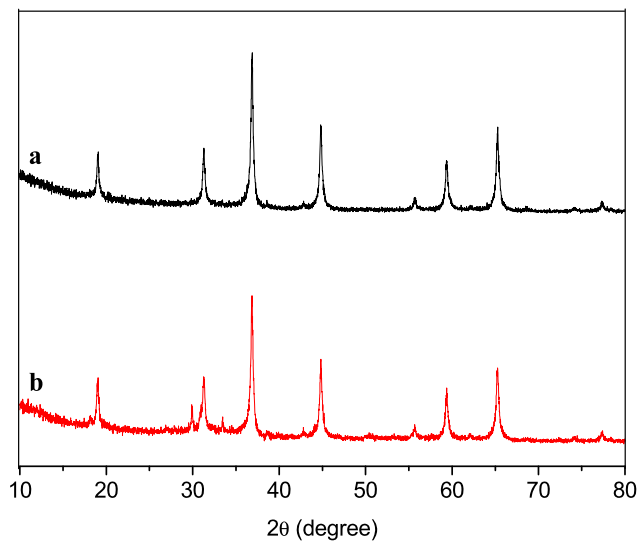
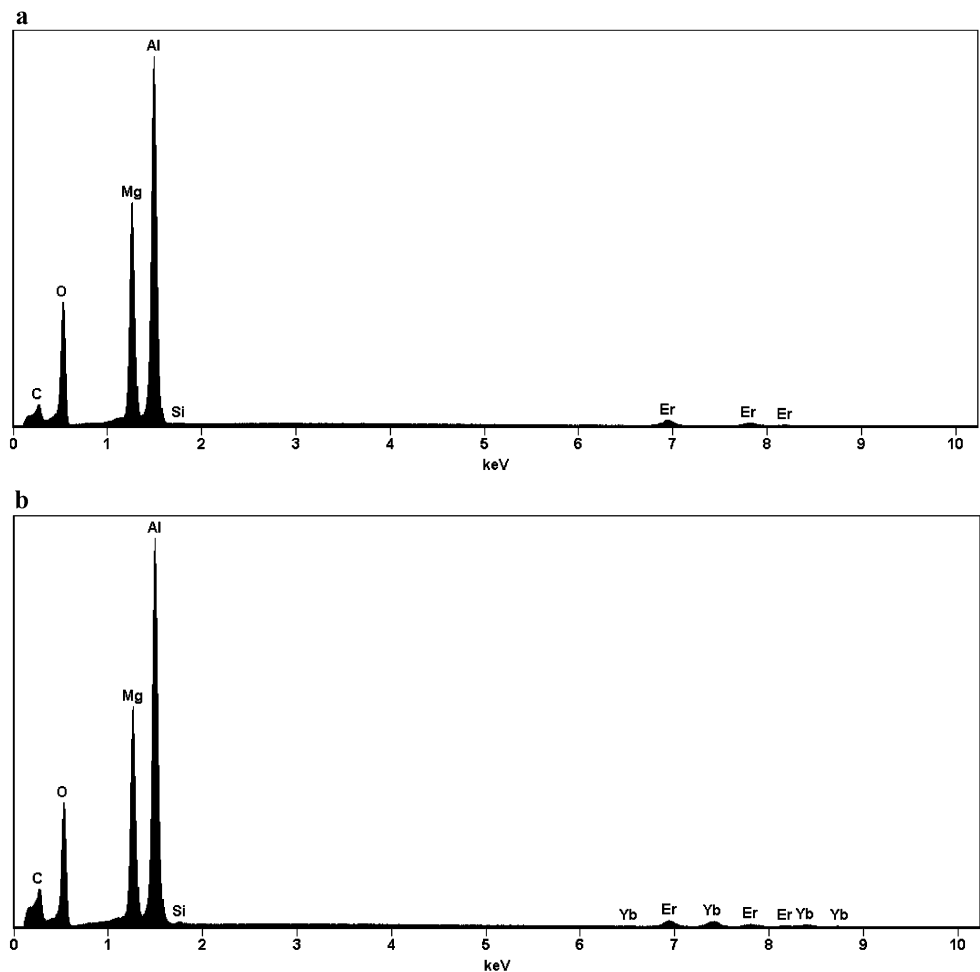


Fig. 1 Powder XRD patterns for (a) $\text{MgAl}_2\text{O}_4:\text{Er}^{3+}$ and (b) $\text{MgAl}_2\text{O}_4:\text{Er}^{3+}, \text{Yb}^{3+}$ phosphor

Fig. 2 EDX spectrum of (a) $\text{MgAl}_2\text{O}_4:\text{Er}^{3+}$ and (b) $\text{MgAl}_2\text{O}_4:\text{Er}^{3+}, \text{Yb}^{3+}$ phosphor

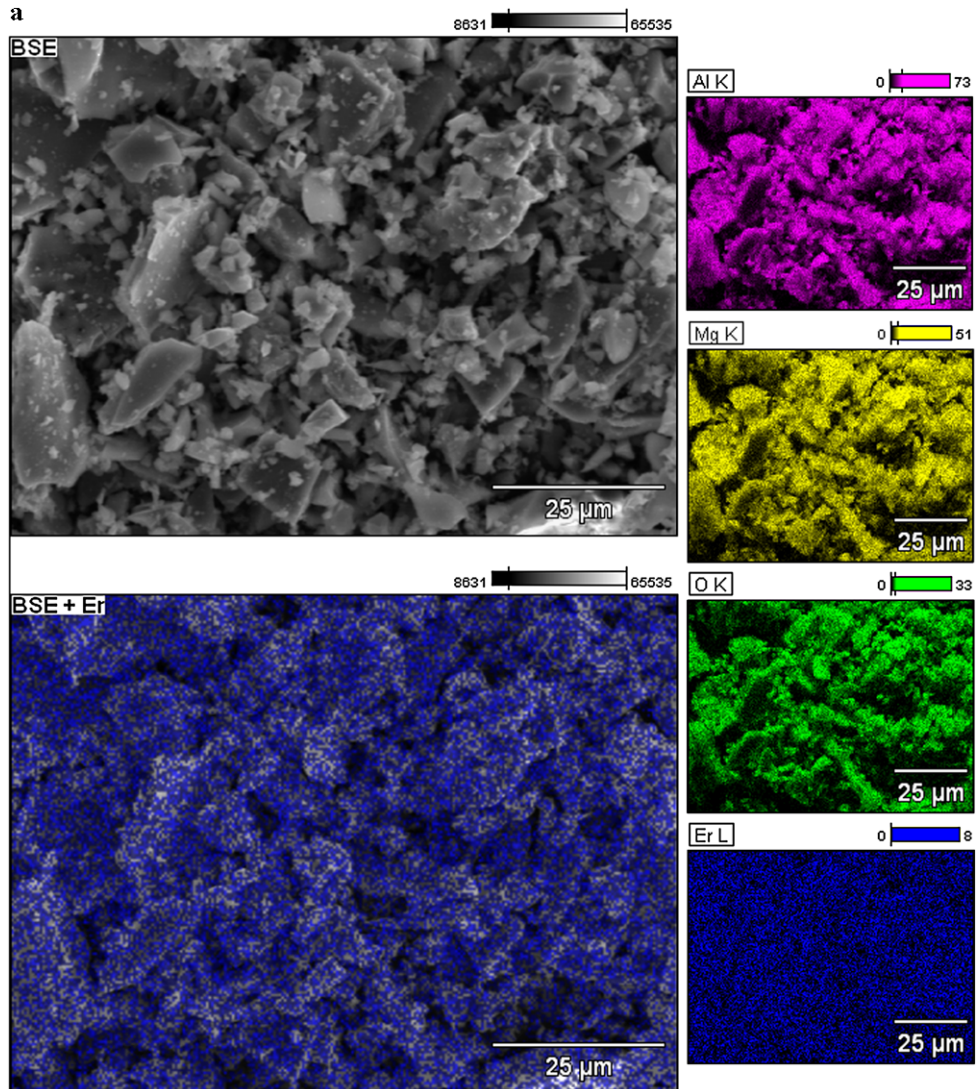


3.2 EDX mapping and spectrum

Figures 2(a) and 2(b) show the EDX spectrum of $\text{MgAl}_2\text{O}_4:\text{Er}^{3+}$ and $\text{MgAl}_2\text{O}_4:\text{Er}^{3+}, \text{Yb}^{3+}$ samples, respectively. In order to confirm the composition of the constituent elements, the entire area of the micrographs (Figs. 3(a) and 3(b), BSE) were analyzed with an EDX spectrum. The EDX analysis indicated the presence of Er, Mg, Al, O in $\text{MgAl}_2\text{O}_4:\text{Er}^{3+}$ phosphor (Fig. 2(a)). On the other hand, the presence of Er, Yb, Mg, Al, O was confirmed in the phosphor $\text{MgAl}_2\text{O}_4:\text{Er}^{3+}, \text{Yb}^{3+}$ (Fig. 2(b)). Besides these peaks, the two EDX spectra show two additional peaks from C and Si. These two peaks are due to the coating and the substrate, respectively.

EDX elemental mappings show the uniform distribution of constituent elements, which indicates a homogeneous distribution of each element in the phosphor powders. Further, in order to know the distribution of Er ions in $\text{MgAl}_2\text{O}_4:\text{Er}^{3+}$ phosphor, the overlapping of BSE

Fig. 3 EDX mapping of (a) $\text{MgAl}_2\text{O}_4:\text{Er}^{3+}$ and (b) $\text{MgAl}_2\text{O}_4:\text{Er}^{3+}, \text{Yb}^{3+}$ phosphor



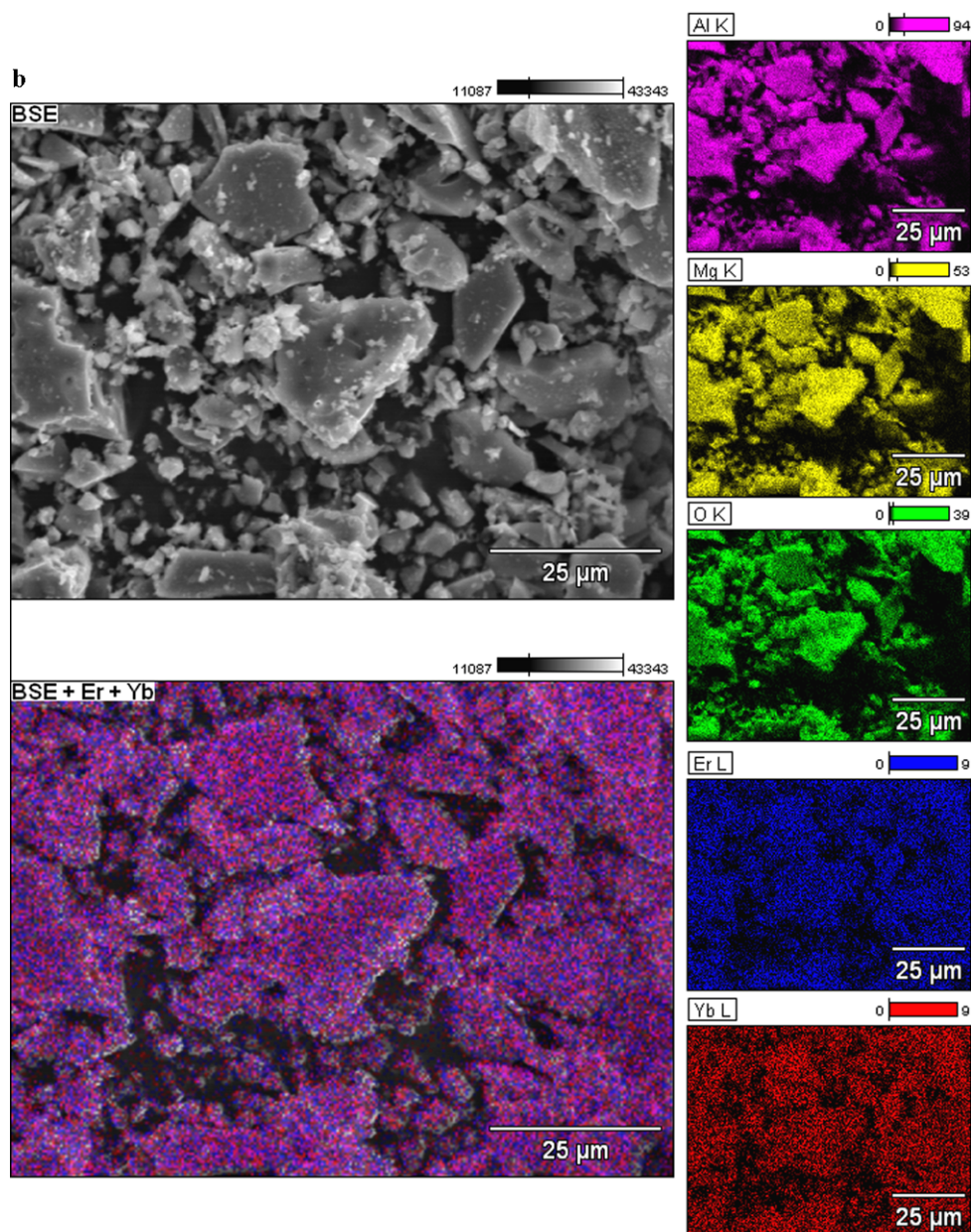
and EDX mapping of Er has been illustrated. This image is shown in Fig. 3(a) (BSE+Er). Similarly, to know the distribution of Er and Yb ions in $\text{MgAl}_2\text{O}_4:\text{Er}^{3+}, \text{Yb}^{3+}$ phosphor, the overlapped image is shown in Fig. 3(b) (BSE+Er+Yb). It is clear from these micrographs that the dopant ions are well dispersed. Finally, EDX mapping and spectrum analysis indicate that there is existence of dopants and they are well dispersed in the MgAl_2O_4 matrix. It is well established that homogeneous distribution of Er^{3+} ions in a matrix plays an important role in order to achieve an efficient amplification [34].

3.3 UV–Visible absorption and photoluminescence of $\text{MgAl}_2\text{O}_4:\text{Er}^{3+}$ phosphor co-doped with Yb^{3+}

The absorption spectrum of $\text{Er}^{3+}/\text{Er}^{3+}-\text{Yb}^{3+}$ doped/co-doped MgAl_2O_4 phosphor powder in the UV–Vis–NIR region is shown in Fig. 4. In the Er^{3+} doped MgAl_2O_4 phosphor, there appear twelve absorption bands correspond-

ing to the ${}^4\text{I}_{15/2}\rightarrow{}^4\text{G}_{9/2}$, ${}^4\text{I}_{15/2}\rightarrow{}^4\text{G}_{11/2}$, ${}^4\text{I}_{15/2}\rightarrow{}^2\text{H}_{9/2}$, ${}^4\text{I}_{15/2}\rightarrow{}^4\text{F}_{3/2}$, ${}^4\text{I}_{15/2}\rightarrow{}^4\text{F}_{5/2}$, ${}^4\text{I}_{15/2}\rightarrow{}^4\text{F}_{7/2}$, ${}^4\text{I}_{15/2}\rightarrow{}^2\text{H}_{11/2}$, ${}^4\text{I}_{15/2}\rightarrow{}^4\text{S}_{3/2}$, ${}^4\text{I}_{15/2}\rightarrow{}^4\text{F}_{9/2}$, ${}^4\text{I}_{15/2}\rightarrow{}^4\text{I}_{9/2}$, ${}^4\text{I}_{15/2}\rightarrow{}^4\text{I}_{11/2}$, and ${}^4\text{I}_{15/2}\rightarrow{}^4\text{I}_{13/2}$ transitions peaking around ~ 366 nm, ~ 378 nm, ~ 407 nm, ~ 442 nm, ~ 451 nm, ~ 488 nm, ~ 521 nm, ~ 543 nm, ~ 653 nm, ~ 797 nm, ~ 976 nm, and ~ 1532 nm, respectively. In the $\text{Er}^{3+}-\text{Yb}^{3+}$ co-doped MgAl_2O_4 phosphor, the peak around ~ 978 nm appears broader compared to that of the $\text{MgAl}_2\text{O}_4:\text{Er}^{3+}$ phosphor. This broadening of the absorption band around ~ 978 nm is due to involvement of both the ${}^2\text{F}_{7/2}\rightarrow{}^2\text{F}_{5/2}$ (Yb^{3+}) and ${}^4\text{I}_{15/2}\rightarrow{}^4\text{I}_{11/2}$ (Er^{3+}) transitions. The larger absorption cross-section corresponding to the ${}^2\text{F}_{7/2}\rightarrow{}^2\text{F}_{5/2}$ transition of Yb^{3+} ion compared to that of the ${}^4\text{I}_{15/2}\rightarrow{}^4\text{I}_{11/2}$ transition of Er^{3+} ion is rather suitable for excitation at ~ 980 nm from the currently available Laser diode source.

Figure 5 shows the photoluminescence spectra of $\text{MgAl}_2\text{O}_4:\text{Er}^{3+}$ and $\text{MgAl}_2\text{O}_4:\text{Er}^{3+}, \text{Yb}^{3+}$ phosphor powders upon excitation with 980 nm from a diode laser in the infrared

Fig. 3 (Continued)

(IR) region. This broadband photoluminescence spectra extending from 1400 nm–1700 nm and peaking at $\sim 1.56 \mu\text{m}$ is attributed to the intra-configurational transition between the first excited (${}^4\text{I}_{13/2}$) and the ground (${}^4\text{I}_{15/2}$) state of Er^{3+} . From this figure, it can be seen that the line shape of PL spectra has no apparent change for the above two phosphor powders with the main peak at about $\sim 1.56 \mu\text{m}$ and a side peak at about $\sim 1.64 \mu\text{m}$ except their relative intensity and FWHM. The effect of alteration in the NIR laser power on the photoluminescence intensity corresponding to the ${}^4\text{I}_{13/2} \rightarrow {}^4\text{I}_{15/2}$ transition has been monitored and presented a linear behavior with the slope $\sim 1.03 \pm 0.02$ and 1.01 ± 0.06 (Fig. 6), respectively, in the $\text{MgAl}_2\text{O}_4:\text{Er}^{3+}$ and

$\text{MgAl}_2\text{O}_4:\text{Er}^{3+},\text{Yb}^{3+}$ phosphor powders. The PL intensity of the peak corresponding to the ${}^4\text{I}_{13/2} \rightarrow {}^4\text{I}_{15/2}$ transition for the $\text{Er}^{3+}-\text{Yb}^{3+}$ co-doped phosphor powders is enhanced by about three times and the corresponding FWHM is increased to about ~ 60 nm compared to that of the $\text{MgAl}_2\text{O}_4:\text{Er}^{3+}$ phosphor powder (FWHM ~ 54 nm). This is an indication of the presence of a strong excitation exchange mechanism between Yb^{3+} and Er^{3+} in the MgAl_2O_4 matrix. This is because of the fact that Yb^{3+} has not only a broader band, but also much larger absorption cross-section than Er^{3+} . In $\text{Er}^{3+}-\text{Yb}^{3+}$ co-doped system, the absorption efficiency of the pump energy is much stronger than those of Er^{3+} doped system. Furthermore, the higher efficiency of energy trans-

Fig. 4 Diffuse reflectance spectrum of (a) $\text{MgAl}_2\text{O}_4:\text{Er}^{3+}$ and (b) $\text{MgAl}_2\text{O}_4:\text{Er}^{3+}, \text{Yb}^{3+}$ phosphor

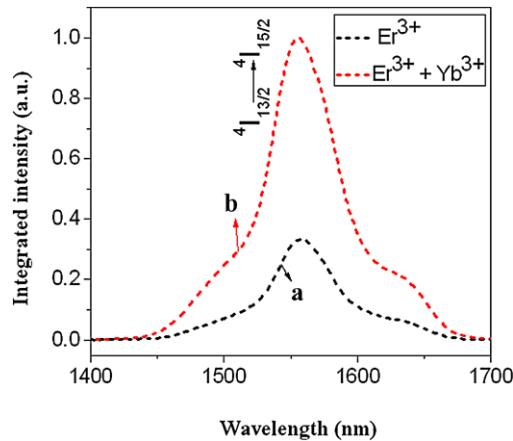
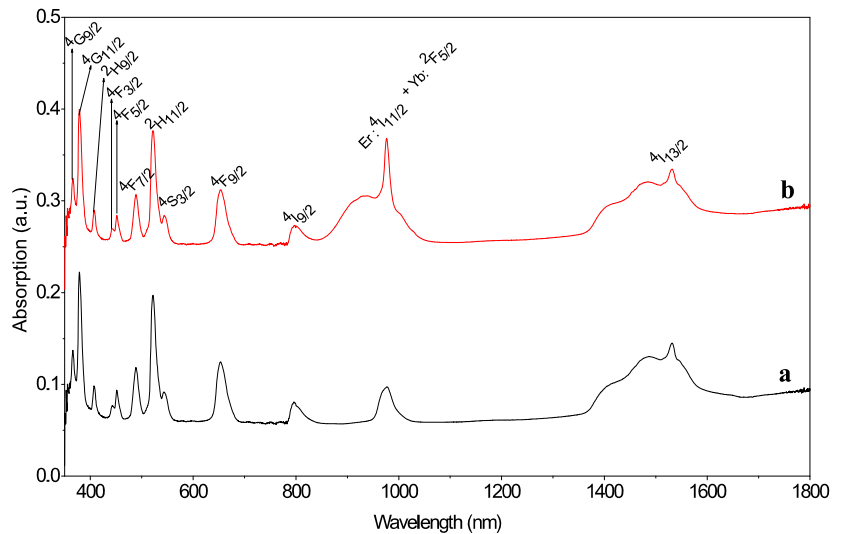


Fig. 5 Photoluminescence spectra of (a) $\text{MgAl}_2\text{O}_4:\text{Er}^{3+}$ and (b) $\text{MgAl}_2\text{O}_4:\text{Er}^{3+}, \text{Yb}^{3+}$ under CW excitation at $\lambda_{\text{exi}} = 980 \text{ nm}$

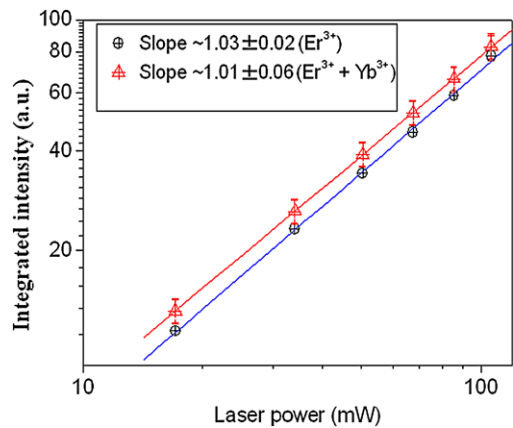


Fig. 6 Variation of the photoluminescence intensity corresponding to the $4I_{13/2} \rightarrow 4I_{15/2}$ transition versus NIR laser intensity

fer from the Yb^{3+} to Er^{3+} has been found in the $\text{Er}^{3+}-\text{Yb}^{3+}$ co-doped system reported elsewhere [34, 35]. The process

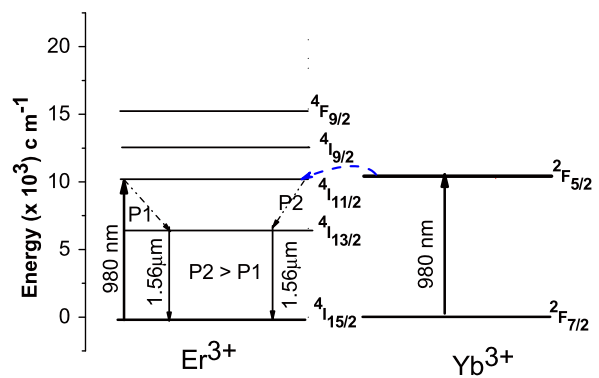


Fig. 7 Energy level diagram of $\text{Er}^{3+}-\text{Yb}^{3+}$

of energy transfer (ET) in $\text{Er}^{3+}-\text{Yb}^{3+}$ system is depicted in Fig. 7. The involvement to the $4I_{13/2}$ level population of Er^{3+} from energy transfer followed by the $2F_{5/2}$ (Yb^{3+}) + $4I_{15/2}$ (Er^{3+}) $\rightarrow 2F_{7/2}$ (Yb^{3+}) + $4I_{15/2}$ (Er^{3+}) {i.e. through process P2} will be much stronger than that given by the process of single Er^{3+} (i.e. direct pumping-through process P1).

The FWHM ($\sim 60 \text{ nm}$) of PL spectra for $\text{Er}^{3+}-\text{Yb}^{3+}$ co-doped MgAl_2O_4 phosphor powder is similar to the FWHM ($\sim 59 \text{ nm}$) reported for the $\text{Er}^{3+}-\text{Yb}^{3+}$ co-doped Al_2O_3 phosphor powder [36]. It is broader than the reported values for Er^{3+} doped materials [32, 37]. It appears that the Yb^{3+} co-doping modifies the local environment of Er^{3+} in MgAl_2O_4 matrix material and enhances the broadening of the FWHM of PL peak in Er^{3+} doped MgAl_2O_4 material [36]. The large optical band width of the PL peak corresponding to the $4I_{13/2} \rightarrow 4I_{15/2}$ transition in $\text{Er}^{3+}-\text{Yb}^{3+}$ co-doped MgAl_2O_4 phosphor powder produced by combustion method makes it a suitable aspirant for the wavelength division multiplexing applications.

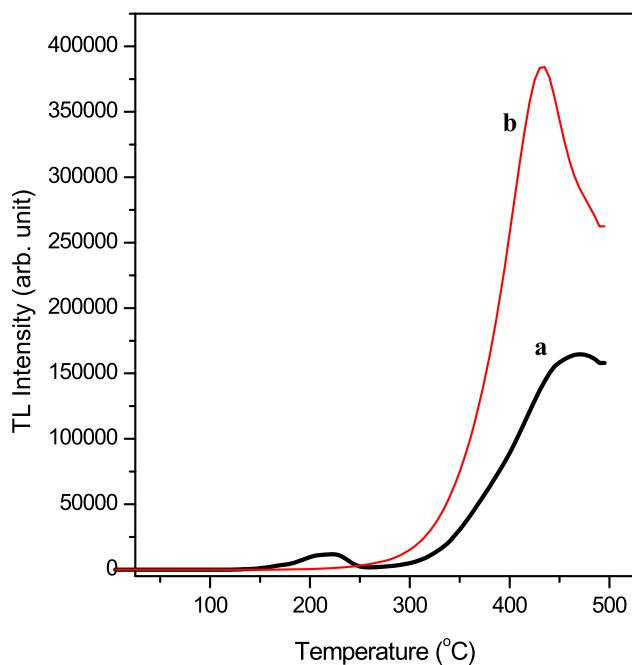


Fig. 8 TSL glow curves of (a) $\text{MgAl}_2\text{O}_4:\text{Er}^{3+}$ and (b) $\text{MgAl}_2\text{O}_4:\text{Er}^{3+}, \text{Yb}^{3+}$ (test gamma dose: 5 Gy)

3.4 TSL and ESR of $\text{MgAl}_2\text{O}_4:\text{Er}^{3+}$ phosphor co-doped with Yb^{3+}

The TSL glow curves of the phosphors MgAl_2O_4 doped with Er^{3+} and $\text{MgAl}_2\text{O}_4:\text{Er}^{3+}, \text{Yb}^{3+}$ are shown in Fig. 8. Two TSL peaks at 210 °C and 460 °C are observed in $\text{MgAl}_2\text{O}_4:\text{Er}^{3+}$ phosphor while only a single peak at 460 °C is seen in $\text{MgAl}_2\text{O}_4:\text{Er}^{3+}, \text{Yb}^{3+}$. In general, Yb^{3+} acts as an efficient sensitizer by transferring a better part of its excitation energy to Er^{3+} . In order to enhance the PL intensity of Er^{3+} in the MgAl_2O_4 sample, the sample is co-doped with Yb^{3+} ions. It is observed that similar to PL emission intensity the TSL intensity is also enhanced significantly with Yb^{3+} co-doping.

The ESR spectrum at room temperature (dose: 5 kGy) of Er^{3+} doped MgAl_2O_4 is shown in Fig. 9. The observed spectrum is a superposition of at least three defect centres and two centres are distinctly seen in the spectrum. This inference is based on thermal annealing experiments. It is possible to identify two centres and these are labeled in Fig. 9. The ESR line labeled as I is due to a centre characterized by a single broad ESR line with an isotropic g-value equal to 2.0114 and 41 gauss linewidth. ESR spectra of Er^{3+} doped MgAl_2O_4 exhibit a large linewidth of centre I indicating an unresolved hyperfine structure. In MgAl_2O_4 , aluminum (^{27}Al) and also magnesium (^{25}Mg) have isotopes with nuclear spin 5/2. ^{27}Al is more abundant (100 %) than ^{25}Mg (10.1 %). Further, its nuclear magnetic moment is higher (3.6385) than that of ^{25}Mg (0.8545) [38]. Hence, the possi-

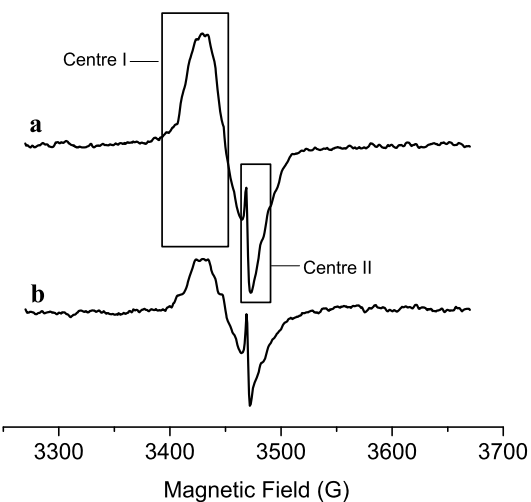


Fig. 9 Room temperature ESR spectra of irradiated (a) $\text{MgAl}_2\text{O}_4:\text{Er}^{3+}$ and (b) $\text{MgAl}_2\text{O}_4:\text{Er}^{3+}, \text{Yb}^{3+}$ phosphor (gamma dose: 5 kGy). Line labeled as I is due to an O^- ion. Centre II line is assigned to a F^+ centre

bility of the electronic spin interaction with aluminum ions is more due to the ion's larger abundance.

MgAl_2O_4 has a face centered cubic lattice of oxygen ions with a lattice parameter of 8.08 Å. It crystallizes in the cubic space group $\text{fd}3\text{m}$ and there are eight molecules in the unit cell. There are 64 tetrahedral symmetry sites and 32 octahedral sites. Natural MgAl_2O_4 has 8 magnesium ions occupying tetrahedral sites and 16 aluminum ions occupying octahedral sites. Synthetic MgAl_2O_4 crystal, on the other hand, can have up to 30 % of cation antisite disorder [39–42]. Numerous trapping sites for the electron and hole on irradiation are created due to antisite formation which results from the interchange of the ions on tetrahedral and octahedral lattice positions by divalent and trivalent ions. Further, defect centres and impurities in the lattice are damaged by irradiation which causes a change in their charge states [43]. These defect centres play a vital role in many of the luminescent and optical properties of the crystal.

Cation disorder and non-stoichiometry of MgAl_2O_4 give rise to a large number of lattice defects, which serve as trapping centres. In this situation, oxygen vacancies should lead to F^+ -centre by trapping electrons after irradiation. On the other hand, hole trapping at aluminum or magnesium vacancies can lead to formation of O^- ions. The observed broad ESR line of centre I and the associated unresolved hyperfine structure indicates that the unpaired electron is delocalized and interacts with nearby aluminum nuclei. Hence, centre I is assigned to an O^- centre stabilized by a nearby cation vacancy (a hole trapped in a $\text{Al}^{3+}/\text{Mg}^{2+}$ ion vacancy). The observed positive g-shift of centre I is also in accordance with the expectations for an O^- ion. It may be mentioned that a similar centre in neutron irradiated MgAl_2O_4 sample has also been ascribed to an O^- ion [44].

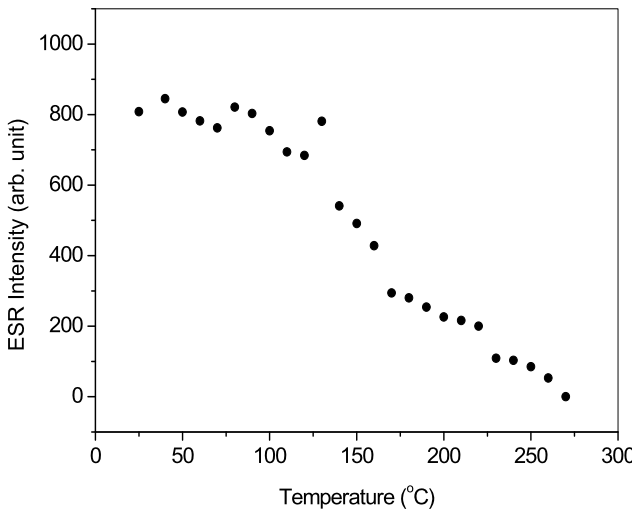


Fig. 10 Thermal annealing behavior of centre I (O^- ion) in $MgAl_2O_4:Er^{3+}$ phosphor

A pulsed-thermal annealing method was used to measure the stability of centre I. After heating the sample up to a given temperature, where it is maintained for 3 minutes, it is cooled rapidly down to room temperature for ESR measurements. Figure 10 shows the thermal annealing behavior of centre I which decays in two stages. The first stage is in the temperature range $100\text{ }^\circ\text{C}$ – $150\text{ }^\circ\text{C}$ and the second stage of decay ($160\text{ }^\circ\text{C}$ – $270\text{ }^\circ\text{C}$) appears to relate to the $210\text{ }^\circ\text{C}$ TSL peak. Two stage decay of centre I shows that it consists of two types of O^- ions (hole trapped in Mg^{2+} or Al^{3+} vacancy) decaying at two different temperature ranges.

Centre II in Fig. 9 is characterized by a single ESR line with an isotropic g-value equal to 2.0044 and 3 gauss linewidth. A likely centre which can be formed after irradiation in this phosphor is F^+ centre (an electron trapped at an anion vacancy). Such a centre was first observed in neutron irradiated LiF [45]. In LiF, a single broad line (linewidth ~ 100 gauss) with a g-factor 2.008 was observed. This centre can also be formed in systems like alkali halides by X-ray or gamma-ray irradiation. F centres are characterized by a small g-shift, which may be positive or negative, a large linewidth (caused due to unresolved hyperfine structure) and saturation properties characteristic of an inhomogeneously broadened ESR line. An anionic vacancy traps an electron during irradiation and such trapping is the basis for the formation of F centres. Hyperfine interaction with the nearest-neighbor cations is the major contribution to the linewidth. Defect centre II formed in the present system is characterized by a small g-shift. The centre also does not exhibit any resolved hyperfine structure. Recently, such a centre was reported in $LiAlO_2$ and $ZnAl_2O_4$ phosphors [46, 47]. On the basis of these observations and considerations of the characteristic features of the defect centres likely to be formed

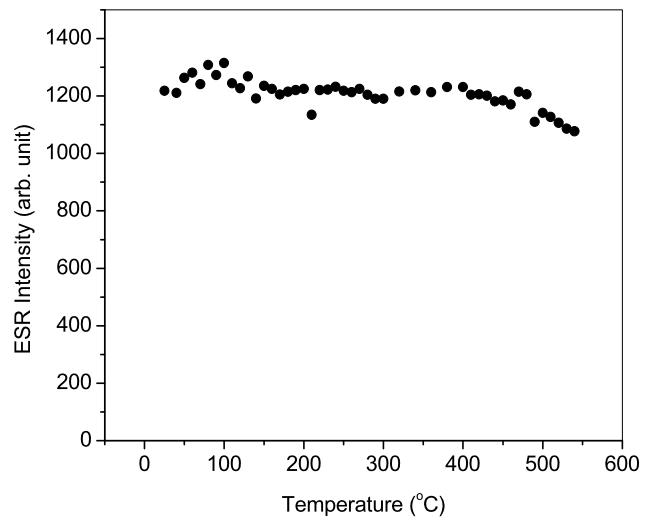


Fig. 11 Thermal annealing behavior of centre II (F^+ centre) in $MgAl_2O_4:Er^{3+}$ phosphor

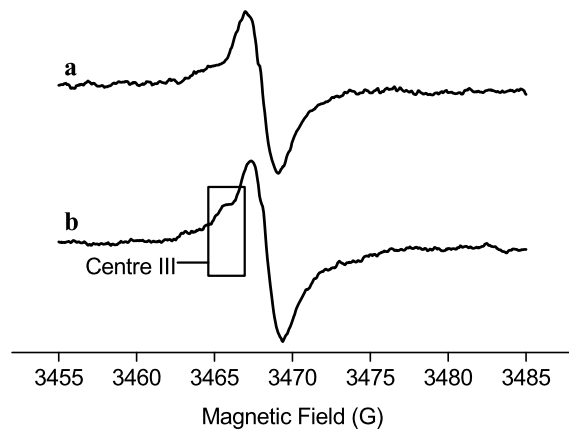


Fig. 12 Room temperature ESR spectra of irradiated $MgAl_2O_4:Er^{3+}$ phosphor. (a) and (b) refer to spectra recorded after annealing at $410\text{ }^\circ\text{C}$ and $540\text{ }^\circ\text{C}$, respectively

in a system such as $MgAl_2O_4:Er^{3+}$, centre II is tentatively assigned to an F^+ centre.

Figure 11 shows the thermal annealing behavior of centre II. It is observed that the centre is highly stable and does not show any indication of decay even at $550\text{ }^\circ\text{C}$. This centre does not appear to be related to the observed TSL peaks in the phosphor.

During the course of thermal annealing experiments, a new centre was observed after the decay of O^- ion (centre I). The corresponding ESR line of this centre could not be seen in the spectrum shown in Fig. 9 due to strong overlap of centre I line. The ESR spectrum after thermal anneal at $410\text{ }^\circ\text{C}$ is shown in Fig. 12 and the new centre, labeled as centre III, appears as a weak shoulder line superposed on centre II. Centre III is also characterized by a single ESR line with an isotropic g-value equal to 2.0058 and 3 gauss

linewidth. It is tentatively assigned to F⁺ centre based on the reasons mentioned above for centre II. The centre appears to decay in the approximate temperature region of the high temperature TSL peak observed in this phosphor. Figure 12 also shows the ESR spectrum recorded after 540 °C thermal anneal and it is observed that centre III has decayed. It is speculated that this F⁺ centre is related to the 460 °C TSL peak observed in the phosphor.

Yb³⁺ co-doped phosphor displays two centres as observed in MgAl₂O₄:Er³⁺. The observed ESR spectrum in the irradiated phosphor at room temperature is shown in Fig. 9(b). Centre I is characterized by a single relatively broad ESR line with an isotropic g-value equal to 2.0162 and 42 gauss linewidth. On the other hand, the ESR line associated with centre II is narrow with a linewidth of 2 gauss and a g-value equal to 2.0042. The two defect centres are assigned to an O⁻ ion and F⁺ centre, respectively, on the basis of the reasons mentioned above. It is to be mentioned that there is a reduction in the yield of O⁻ ions by about 50 % in Yb co-doped phosphor. It is very likely that the absence of low temperature TSL peak in the co-doped phosphor could be related to this reduction in the concentration of O⁻ ions.

4 Conclusions

MgAl₂O₄:Er³⁺ and MgAl₂O₄:Er³⁺,Yb³⁺ phosphors are prepared by combustion synthesis. It is noted that the photoluminescence intensity corresponding to the $^4I_{13/2} \rightarrow ^4I_{15/2}$ transition in Er³⁺-Yb³⁺ co-doped phosphor powder is enhanced by about three times due to the occurrence of a strong excitation energy transfer from Yb³⁺ to Er³⁺ in the MgAl₂O₄ matrix. The coherent effect of Er³⁺-Yb³⁺ co-doping on increased FWHM to about ~60 nm compared to that of the MgAl₂O₄:Er³⁺ phosphor powder (FWHM ~54 nm) has been seen and hence makes the present material suitable for wavelength division multiplexing applications. Also, two TSL peaks are observed at 210 °C and 460 °C in MgAl₂O₄:Er³⁺ phosphor while only the high temperature peak is seen in the co-doped phosphor. Three defect centres are identified in irradiated MgAl₂O₄:Er³⁺ phosphor and these centres are assigned to O⁻ ion and F⁺ centres. O⁻ ion (hole centre) appears to correlate with the 210 °C TSL peak while one of the F⁺ centres appears to be related to the TSL peak at 460 °C.

Acknowledgements Dr. Vijay Singh expresses his thanks to the support of the Hanse-Wissenschaftskolleg, Delmenhorst, Germany. Y.D. Jho acknowledges the support from Fusion-Tech. Developments for THz Info. & Comm. Program of GIST. T. K. Gundu Rao is grateful to FAPESP, Brazil, for the research fellowship.

References

- D. Jia, W.M. Yen, *J. Lumin.* **101**, 115 (2003)
- I. Omkaram, G. Seeta Rama Raju, S. Buddhudu, *J. Phys. Chem. Solids* **69**, 2066 (2008)
- V. Singh, M.D. Masuque Haque, D.-K. Kim, *Bull. Korean Chem. Soc.* **28**, 2477 (2007)
- A.S. Maia, R. Stefani, C.A. Kodaira, M.C.F.C. Felinto, E.E.S. Teotonio, H.F. Brito, *Opt. Mater.* **31**, 440 (2008)
- L.R.P. Kassab, F.A. Bomfim, J.R. Martinelli, N.U. Wetter, J.J. Neto, C.B. de Araújo, *Appl. Phys. B* **94**, 239 (2009)
- H.C. Seat, J.H. Sharp, *Meas. Sci. Technol.* **14**, 279 (2003)
- J. Yang, S. Xiao, J. Ding, X. Yang, X. Wang, *J. Alloys Compd.* **474**, 424 (2009)
- O. Pérón, C. Duverger-Arfuso, Y. Jestin, B. Boulard, M. Ferrari, *Opt. Mater.* **31**, 1288 (2009)
- X. Wang, Q. Nie, T. Xu, X. Shen, S. Dai, N. Gai, Y. Zhou, *Spectrochim. Acta, Part A* **72**, 543 (2009)
- M. Liu, S. Wang, D. Tang, L. Chen, J. Ma, *J. Rare Earths* **27**, 66 (2009)
- D. Solís, T. López-Luke, E. De la Rosa, P. Salas, C. Angeles-Chavez, *J. Lumin.* **129**, 449 (2009)
- W. You, Y. Huang, Y. Chen, Y. Lin, Z. Luo, *Opt. Commun.* **281**, 4936 (2008)
- B. Dong, C.R. Li, M.K. Lei, *J. Lumin.* **126**, 441 (2007)
- C. Li, B. Dong, S. Li, C. Song, *Chem. Phys. Lett.* **443**, 426 (2007)
- X.Y. Chen, C. Ma, Z.J. Zhang, X.X. Li, *Microporous Mesoporous Mater.* **123**, 202 (2009)
- P. Głuchowski, R. Pażik, D. Hreniak, W. Stręk, *Chem. Phys.* **358**, 52 (2009)
- J.M.G. Tijero, A. Ibarra, *J. Phys. Chem. Solids* **54**, 203 (1993)
- V. Singh, R.P.S. Chakradhar, J.L. Rao, D.-K. Kim, *J. Solid State Chem.* **180**, 2067 (2007)
- P. Lombard, B. Boizot, N. Ollier, A. Jouini, A. Yoshikawa, *J. Cryst. Growth* **311**, 899 (2009)
- T. Böttger, G.J. Pryde, C.W. Thiel, R.L. Cone, *J. Lumin.* **127**, 83 (2007)
- H. Chen, Y.H. Liu, Y.F. Zhou, Q.Y. Zhang, Z.H. Jiang, *J. Non-Cryst. Solids* **351**, 3060 (2005)
- S. Hocdé, S. Jiang, X. Peng, N. Peyghambarian, T. Luo, M. Morell, *Opt. Mater.* **25**, 149 (2004)
- W. Deng, J. Zhang, J. Sun, Y. Luo, J. Lin, X. Wang, W. Xu, *J. Non-Cryst. Solids* **336**, 44 (2004)
- S.J. Dhoble, S.V. Moharil, T.K. Gundu Rao, *J. Lumin.* **126**, 383 (2007)
- S. Murali, V. Natarajan, T.K. Seshagiri, R.M. Kadam, R. Venkataramani, M.D. Sastry, *Radiat. Meas.* **37**, 259 (2003)
- V. Natarajan, T.K. Seshagiri, R.M. Kadam, M.D. Sastry, *Radiat. Meas.* **35**, 361 (2002)
- S.J. Dhoble, S.V. Moharil, T.K. Gundu Rao, *J. Lumin.* **93**, 43 (2001)
- N.K. Porwal, R.M. Kadam, T.K. Seshagiri, V. Natarajan, A.R. Dhopale, A.G. Page, *Radiat. Meas.* **40**, 69 (2005)
- V. Singh, T.K. Gundu Rao, *J. Solid State Chem.* **181**, 1387 (2008)
- V. Singh, T.K. Gundu Rao, J.-J. Zhu, *J. Lumin.* **128**, 583 (2008)
- V. Singh, J.-J. Zhu, T.K. Gundu Rao, M. Tiwari, P.H. Cheng, *Chin. Phys. Lett.* **22**, 3182 (2005)
- V. Singh, V. Kumar Rai, I. Ledoux-Rak, S. Watanabe, T.K. Gundu Rao, J.F.D. Chubaci, L. Badie, F. Pelle, S. Ivanova, *J. Phys. D, Appl. Phys.* **42**, 065104 (2009)
- M. Pošarac, A. Devečerski, T. Volkov-Husović, B. Matović, D.M. Minić, *Sci. Sinter.* **41**, 75 (2009)
- L. Zhang, H.F. Hu, C.H. Qi, F.Y. Lin, *Opt. Mater.* **17**, 371 (2001)
- V. Singh, V. Kumar Rai, I. Ledoux-Rak, H.-Y. Kwak, *Appl. Phys. B* **97**, 103 (2009)
- X.J. Wang, M.K. Lei, T. Yang, B.S. Cao, *Opt. Mater.* **26**, 253 (2004)
- G.N. van den Hoven, E. Snoek, A. Polman, *Appl. Phys. Lett.* **62**, 3065 (1993)

38. R.C. Weast (ed.), *Handbook of Chemistry and Physics* (CRC, Cleveland, 1971)
39. T.J. Grey, in *High Temperature Oxides*, ed. by A.M. Alper (Academic, New York, 1971) (Pt. IV)
40. U. Schmocke, H.R. Boesch, F. Waldner, Phys. Lett. A **40**, 237 (1972)
41. G.E. Bacon, Acta Crystallogr. **5**, 684 (1952)
42. E. Stoll, P. Fischaer, W. Haig, G. Maier, J. Phys. (Paris) **25**, 447 (1964)
43. G.P. Summers, G.S. White, K.H. Lee, J.H. Crawford, Phys. Rev. B **21**, 2578 (1980)
44. V.T. Gritsyna, V.A. Kobyakov, Zh. Tekh. Fiz. **55**, 354 (1985) [Sov. Phys. Tech. Phys. **30**, 206 (1985)]
45. C.A. Hutchison, Phys. Rev. **75**, 1769 (1949)
46. B. Dhabekar, E. Alagu Raja, S. Menon, T.K. Gundu Rao, R.K. Kher, B.C. Bhatt, Rad. Meas. **43**, 291 (2008)
47. S. Menon, B. Dhabekar, E. Alagu Raja, S.P. More, T.K. Gundu Rao, R.K. Kher, J. Lumin. **128**, 1673 (2008)